Forward Magnetic Scattering Amplitude of Iron for Thermal Neutrons*

C. S. Schneider† and C. G. Shull
Massachusetts Institute of Technology, Cambridge, Massachusetts 02139
(Received 19 October 1970)

The forward magnetic scattering amplitude of iron for thermal neutrons was determined on an absolute scale in two different experiments: the refractive bending of a polarized neutron beam by a small-angle prism (apex angle 32°) and the refractive bending of an unpolarized neutron beam by a large-angle biprism (apex angle 150°) of polycrystalline iron magnetized to saturation. This magnetic scattering amplitude, determined at 301 °K, was established as being $0.589(6)\times10^{-12}$ cm/atom and is in excellent agreement with the value of $0.587(<1)\times10^{-12}$ cm/atom that is calculated from magnetization measurements. The measurement confirms the discrepancy between this value and that extrapolated by a $3d$-electron form factor from earlier Bragg reflection measurements, namely 0.645×10^{-12} cm/atom, and this supports the presence of an anomalous magnetic form factor in iron at scattering angles smaller than permitted in Bragg reflection. Simultaneous measurement of the nuclear scattering amplitude yielded $0.954(6)\times10^{-12}$ cm/atom in good agreement with previous powder measurements. The small refractive bending angles over a range of 20 sec of arc were measured by placing the prisms between the crystals of a double perfect-crystal spectrometer with torsion goniometer control.

I. INTRODUCTION

The forward magnetic scattering amplitude of an atom for neutrons is thought to be related to its total magnetic moment, according to neutron magnetic scattering theory, by the equation

$$p_0=(2M_n\mu_n/\hbar^2)\,\mu_a\ , \tag{1}$$

where M_n is the neutron mass, μ_n is its magnetic moment, and μ_a is the atomic magnetic moment. Measurements of the magnetization and atomic densities can then be used to calculate the atomic magnetic moment and then the forward magnetic scattering amplitude; in the case of iron, this yielded 0.587×10^{-12} cm/atom. In 1961, however, direct measurement of the magnetic scattering amplitudes of iron[2] for all of the Bragg reflections from the (110) to the (622) planes yielded information which indicated a forward magnetic scattering amplitude of 0.645×10^{-12} cm/atom by extrapolating the measured amplitudes at the Bragg reflections using a theoretical $3d$-electron form factor. This form factor showed very excellent agreement with every measured amplitude when normalized for best agreement and corrected for the effects of spatial asymmetry of the atoms in the crystal. The source of the discrepancy then lay in the significance of the forward scattering amplitude.

In the usual interpretation of diffracted neutron intensities, the collection of discrete measured amplitudes is an incomplete set of coefficients in the infinite Fourier sum which completely describes the spin density in the unit cell; thus

$$\rho(\vec{r})=\frac{1}{V}\sum_{hkl}F_{hkl}\,e^{-i\vec{K}_{hkl}\cdot\vec{r}}\ , \tag{2}$$

where V is the volume of the unit cell and F_{hkl} is the structure amplitude for the reflection (hkl),

$$F_{hkl}=\sum_{\alpha}p_{hkl}\,e^{i\vec{K}_{hkl}\cdot\vec{R}_\alpha}\ , \tag{3}$$

for scattering perpendicular to the magnetization axis. The forward amplitude p_{000}, denoted p_0, thus corresponds to a constant density in the sum. The excellent fit to the theoretical $3d$-electron form factor away from the forward reflection implies that any non-$3d$ spin density must be extended relative to the nuclear position so that its structure amplitude contribution is negligible for all nonforward Bragg reflections. Indeed, recent calculations[3-5] have suggested the presence of a uniform negative spin density due to the exchange interaction of the $4s$ electrons with the unpaired $3d$ electrons. An experimental measurement of the forward magnetic scattering amplitude would not determine the specific quantum state of the polarized electrons but would confirm the presence of the non-$3d$ spin-density contribution. It was the object of this experiment to directly measure this amplitude in a neutron scattering experiment.

A study of the magnetic refractive index of materials for neutrons represents one method for determining the forward magnetic scattering amplitude. Three effects associated with the refractive index were considered by the authors: total reflection from a mirror surface, refractive small-angle scattering in a physically or magnetically inhomogeneous sample, and prism refraction. The first, total reflection, occurs when a beam is incident upon a polished surface at angles less than the critical angle, which is usually a few minutes of arc for thermal neutrons. Surface preparation, neutron

depolarization, and angular resolution can lead to difficulties which offset the simplicity of the apparatus. Small-angle scattering effects depend upon the size and shape of the inhomogeneities, parameters which cannot be accurately determined using presently known preparation or measurement techniques. The third effect, prism refraction, involves bending a neutron beam through very small angles, some sec of arc, the deflection depending upon the neutron wavelength and the prism apex angle as well as the scattering amplitude. This prism refraction technique, first developed for neutrons in this laboratory, has been shown capable of producing quantitative results for nonmagnetic media; it was chosen as the method for determining the magnetic refractive index of iron.

The dependence of the refractive index upon the forward scattering amplitude has been derived by Goldberger and Seitz[6] following the techniques of the dynamical theory of x-ray diffraction for the case in which only the forward wave is significant. The extension of this analysis to the case of magnetic materials has been discussed by Halpern, Hamermesh, and Johnson[7] among others in which the refractive index for a monoatomic material can be written with sufficient accuracy as

$$n = 1 - (N\lambda^2/2\pi)(b \pm p_0) \ , \qquad (4)$$

where N is the atomic density, λ is the neutron wavelength, and b and p_0 are the coherent nuclear and forward magnetic scattering amplitudes, respectively. The two values of the refractive index correspond to the two states of neutron polarization relative to the magnetization direction. Imaginary components of the scattering amplitudes can be safely ignored for the case of present interest since negligible effects on the refractive index are involved. As with x radiation, the numerical size of the terms in Eq. (4) yields values of n which differ from unity by only a few parts per 10^5.

The refractive bending of a neutron beam by an iron prism is calculated from Fermat's principle once the refractive index is known: the minimum optical path is one of refractive bending angle

$$\Delta\theta = (N\lambda^2/\pi)(b \pm p_0)(1 + \epsilon^2 \sec^2\tfrac{1}{2}\phi) \tan\tfrac{1}{2}\phi \ , \qquad (5)$$

where ϕ is the full apex angle of the prism and ϵ is the angular tip of the prism about its apex edge from the symmetrical passage orientation. The minimum, at symmetrical passage, was established by rocking the prism about its apex edge and finding the center of the parabolic deflection curve. Effects due to rotational tipping of the prism about other axes should also enter into this equation but these were readily made negligible in the present experiment and will not be introduced. With the neutron wavelength and iron prism angles used in the present experiment the deflection angles of Eq. (5) range up to 15 sec of arc.

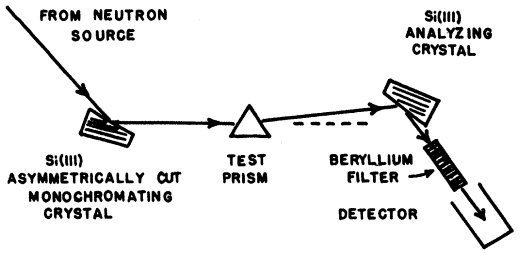

FIG. 1. Schematic diagram of double-crystal spectrometer used in determining prism refractive bending.

II. EXPERIMENT

The experimental apparatus, which is shown in Fig. 1, exploits the high-angular resolution of a double perfect-crystal spectrometer. Using the (111) reflection of two perfect silicon crystals whose surfaces were cut 11° away from the planes (see later discussion), the full width at half-maximum (FWHM) intensity in rocking the analyzer crystal through the reflection was found to agree very closely with the calculated width (see below) when the crystals were aligned parallel about the horizontal tipping axis. The neutrons were reflected from the monochromator crystal at a mean Bragg angle of 22° 26′ over ranges from 15 to 30 min of arc, corresponding to wavelength bands of 0.04 and 0.08 Å about a mean of 2.393(3) Å.[8]

The dynamical theory of diffraction predicts the angular dependence of the reflectivity of one neutron ray from a perfect crystal. Finite-beam collimation does not increase the rocking width of the analyzer above that for a single ray when crystals of identical planar spacing are used in the parallel mode, as in this experiment, for the beam in a double perfect-crystal spectrometer exhibits the property of perfect dispersion, which allows its nearly total reflection over a few sec of arc. Each of the silicon crystals exhibits total reflectivity over an angular range of

$$\omega_D = \frac{N\lambda^2 F_{111}}{4\pi \sin 2\theta_B} \left(\frac{\sin(\theta_B - \chi)}{\sin(\theta_B + \chi)}\right)^{1/2} \ , \qquad (6)$$

where F_{111} is the structure amplitude for the (111) reflection, and $\chi = 11°$ is the asymmetry cut angle. The convolution of these two reflectivities yields a nearly triangular reflectivity whose FWHM is increased by a factor of 1.39 to a width of 1.32 sec of arc for the present experimental conditions. Misalignment of the two crystals about the horizontal axis in the reflecting plane, however, causes a broadening by

$$\omega_B = \tfrac{1}{2}\xi^2 \beta_H \sec^2\theta_B \ , \qquad (7)$$

where ξ is the angle of misalignment, θ_B is the Bragg angle, and β_H is the horizontal collimation width. It was necessary to have the alignment correct within 10 min of arc to insure negligible broadening in the rocking width. Due to the lattice structure of the silicon crystals, the (333), (444), and further high-order reflections were present. These affect both the symmetry and width of the unrefracted rocking curve as well as the refractive angle measurements. These effects were made negligible by passing the neutron beam through 6 cm of Be single crystal oriented so that the small wavelengths were sharply reduced while the primary wavelength was largely unattenuated. Certain orientations about the normal to the reflecting plane allow simultaneous Bragg reflections to occur in the silicon crystals – these were calculated in advance and an orientation was selected for the wavelength used which permitted only the primary reflection. Proper care to minimize the effects of misalignment and higher-order reflections lead to an analyzer rocking width in excellent agreement with the calculated width of 1.32 sec of arc.

The analyzer crystal was found to have a strain curvature arising presumably from its mode of support such that the relative orientation of the reflecting planes varied by about 0.20 sec of arc across the crystal face. This distortion originally necessitated corrections to the small-angle prism data since prism reversal introduced a shift in the beam position by preferential attenuation. By restricting the beam to a centered flat region of the crystal, however, the correction was reduced to less than 0.01 sec of arc.

The Bragg angle varies with the analyzer planar spacing, which is subject to thermal expansion; the calculated shift in proper orientation of the analyzer relative to the monochromator is 0.24 sec of arc/°C temperature difference between the two crystals. In order to reduce thermal drifting, the spectrometer was surrounded by thermal lagging and kept in a constant temperature room maintained at 28 °C within 0.1 °C. This precaution did not entirely eliminate drifting, however; variations of the analyzer reflectivity indicated that there were daily changes arising probably from strains in the reactor building floor due to outside atmospheric conditions, as well as weekly changes associated with the reactor operational schedule. The crystals in the spectrometer were separated by the sizable distance of 3.5 m because of the size of the necessary shielding, the beam polarizing equipment, and the electromagnet for magnetizing the test prisms. This necessitated separate mounting of the two crystals from the floor and consequent sensitivity to small floor strains. Because these driftings were generally of long period, they could be eliminated by a suitable procedure of data accumulation as discussed later.

Control of the analyzer crystal was achieved using a torsion goniometer, a device capable of reproducing angular orientations within 0.01 sec of arc by adjusting the torque on a vertical column.[9] In this experiment the torque was controlled with a two-stage mechanism: by adjusting the deflection of a cantilever bending strip with a micrometer at one end, a fine motion near the other fixed end was produced and transmitted to a rigid torsion arm by means of a small steel ball bearing against a polished carborundum rod. This fine translation caused the rotation of the torsion column at the other end of the torsion arm. The steel ball-bearing surface, although sufficient for the accuracy of the present determination, caused fluctuations during repositioning of the micrometer of about 0.01 sec of arc. Calibration of the torsion goniometer was carried out by measuring the angular deflection with an optical interferometer mounted on a rigid arm extending 6 in. away from the torsion column axis. The deflection was measured with the arm in all four orthogonal orientations about the torsion axis, yielding two calibrations by averaging opposing deflections. Cantilever deflection of the torsion column due to the applied force amounted to 1% with the rigid arm parallel to the torsion arm; a 5% cantilever bending effect was observed in the perpendicular mode corresponding to vertical travel of the ball-bearing contact point. The two calibrations, which are shown in Fig. 2, do agree within 1%, and were averaged for calculating the deflections.

A first set of prisms was formed from a pure iron single crystal to exploit the small attenuation when the prism-crystal was oriented away from Bragg reflections. These crystals were prepared by a strain-anneal growth method rather than by conventional cooling from the melt because of the γ-α phase transformation at 910 °C, which is below the melting point. Transmission of a neutron beam

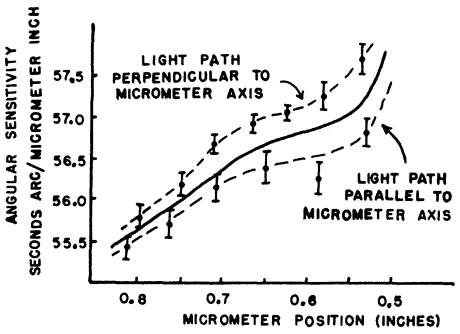

FIG. 2. Angular sensitivity of analyzing crystal goniometer as calibrated in two modes with sodium light interference fringes.

through a magnetically saturated sample showed considerable small-angle scattering over several sec of arc, presumably arising from physical inhomogeneities in the crystal; this was troublesome because it hindered the interpretation of the small refractive bending effects. Subsequent studies of polycrystalline pure iron samples showed considerably less broadening; hence it was decided to use prisms fabricated from polycrystalline iron.

The analysis of the prism chemical composition showed a total of 0.3 at.% impurities (mainly Cu, Mn, C, and Ni). From the polycrystalline iron a prism of 32° apex angle was formed as well as five prisms having 150° apex angles. The large-angle biprisms were used with an incident unpolarized neutron beam, producing two well-separated spin state peaks for each half of the biprisms. The orientation of the small-angle prism was repeatedly reversed in a beam whose polarization was nearly complete due to the angular separation effected with a double set of 120° polarizing prisms. These two independent experimental modes are sketched in Fig. 3. The material used to form the polarizing prisms was monocrystalline iron stabilized with 3.8 wt% silicon to allow cooling from the melt. The polarizing prisms were magnetized in a permanent magnet field of 5 kOe and did not show appreciable small-angle broadening effects. The test prisms were magnetized within the gap of an electromagnet with field strength of 11.6 kOe.

Physical dimensions of the prisms were kept small to avoid large attenuation. Each prism was 1 in. in length and roughly $\frac{1}{4}$ in. at its base (along the beam). The small-angle prism was about $\frac{1}{4}$ in. wide while the other prisms were about $\frac{1}{16}$ in. wide. In order to accept more neutrons, these thinner large-angle prisms were cascaded, five wide for the 150° prisms and three wide for the 120° polarizing prisms. Each of the three prism sets was held firmly in an aluminum box, open at top and bottom to allow prism contact with the magnet poles, and containing a sheet of 0.040-in. Cd across the beam, with a window to define the neutron path.

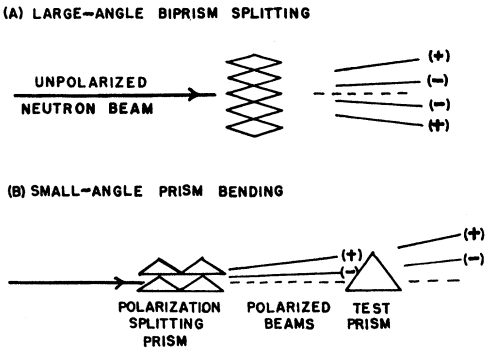

FIG. 3. Methods used in determining magnetic refractive bending of a neutron beam. In method (B) the angular shift of the polarized beam components is measured upon inversion of the test prism. The algebraic signs designate the spin state of the transmitted beam components.

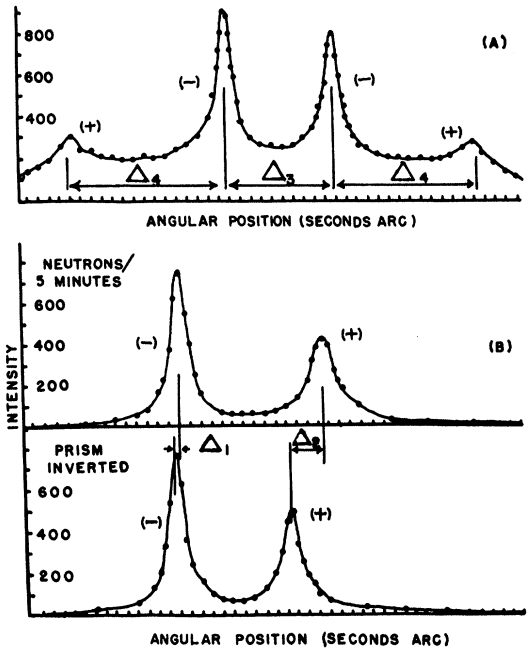

FIG. 4. Split beam patterns obtained through (A) large-angle biprism with unpolarized incident beam and (B) small-angle prism with preseparated polarized beam components.

Determination of the prism apex angles was made using an optical goniometer accurate to within 1 min of arc. Inspection of the surface flatness showed variations of 3 min of arc over the surface, yielding a mean value for the small prism apex angle of $31°56(2)'$. The large-angle prism apex angles varied by 10 min on either side of a mean of $150°28(3)'$; these variations produced sufficiently small refractive broadening that the mean apex angle corresponded to the mean refracted angle.

Measurements of the refractive bending angles were made by observing the neutron intensity reflected from the analyzer crystal as a function of its orientation. These analyzer rocking curves, shown in Fig. 4 for the three prism configurations, were analyzed to extract the refraction angles. A peak center is generally the center of the *integrated intensity*; when the peak is symmetric, however, this center becomes the point midway between two points of equal intensity. Symmetry of the unrefracted beam peak was checked and found to hold within 0.01 sec of arc over a range of 2 sec of arc either side of the peak center. The symmetry of the peaks produced by the polarizing prisms was

equally excellent out to the region where overlap effects became significant. In order to minimize the instrumental drifting effects mentioned earlier, the peak separations in Fig. 4(A) and their shift with prism reversal in Fig. 4(B) were determined by a step-sampling procedure rather than by a slow continuous scanning over the peak spectrum. In this method, two nearly symmetric intensity-angular position points would be determined on one peak followed immediately by a similar sampling on the second peak and this procedure would be cycled many times with the sampling occuring over different intensity regions of the peaks. Uniform drifting could be eliminated in this way.

We notice in the spin-splitting pattern of Fig. 4(A) that the peak widths are spin dependent, indicative of a spin-dependent small-angle scattering. This was studied independently in some detail by studying the broadening after passage of polarized beam components through plate samples as a function of magnetization. The broadening was found to become independent of field strength for fields above 3 kOe (well below that applied during the prism refraction studies) with severe broadening setting in at lower field strengths. This suggested that the high-field strength broadening originated in refractive broadening by nonmagnetic clusters with consequent sensitivity to the neutron polarization. Indeed estimates of the degree of broadening using observations on etch-pit density and size and from precision density measurements gave results in agreement with what was observed. For low-field strengths the presence of magnetic domain structure is expected to cause severe broadening and loss of intensity.

III. CORRECTIONS

Deviations from the ideal experiment included three effects: spin depolarization, refraction in the magnetizing fields, and chemical impurities. Of these the depolarization correction was the most significant, still amounting to less than 2% in all cases.

Neutron depolarization within the prisms results from the magnetic irregularities of incompletely aligned domains. In addition, external depolarization can arise from stray magnetic fields in the experimental environment. Both of these sources would cause discrete depolarization peaks in the observed analyzer rocking curves, requiring data corrections depending upon both the depolarization peak intensities and their separation from the primary peaks. Depolarization effects within the large-angle prisms were determined together with other intensity corrections by analyzing the shape of the peaks in the rocking curve. Because the large-angle prism experiments were carried out with unpolarized incident radiation there is no correction for external depolarization. Upon entering the prism, however, polarized components are produced which then may suffer internal polarization changes thereby affecting the emergent beam pattern.

These internal depolarization effects were treated by extrapolating to infinite field the primary peak separations from 1.8- to 11.6-kOe magnetizing field (the dependence of depolarization upon the applied field in polycrystalline iron was found to be $H^{-1.0}$ using 1.04-Å wavelength neutrons in a conventional polarized neutron spectrometer). This internal spin depolarization was probably less than 1% as suggested by the shape of the rocking curve due to transmission through only these prisms. For the small-angle prism experiments both external and internal depolarization must be considered. External depolarization between the polarizing prisms and the small-angle prism was observed to be similarly low from the rocking curve taken with the two sets of polarizing prisms separated: One remained in the permanent magnet while the other was placed in the electromagnet. Previous experience with guide fields such as used between the polarizing and sample prisms suggested a depolarization less than $\frac{1}{10}$%. External depolarization effects were accordingly neglected.

The refraction of neutrons in a pure magnetic

TABLE I. Summary of experimental measurements for the magnetic prism deflection of a neutron beam.

Deflection[a]	Measured angular separation (sec of arc)	Corrected angular separation (sec of arc)	Effective scattering amplitude (10^{-12} cm/atom)
$\Delta_1 = 4(N\lambda^2/2\pi)\,(b-p_0)\tan\frac{1}{2}\phi_1$	0.653(12)	0.655(12)	0.365(7)
$\Delta_2 = 4(N\lambda^2/2\pi)\,(b+p_0)\tan\frac{1}{2}\phi_1$	2.809(18)	2.818(18)	1.545(10)
$\Delta_3 = 4(N\lambda^2/2\pi)\,(b-p_0)\tan\frac{1}{2}\phi_2$	8.98(5)	8.94(6)	0.369(3)
$\Delta_4 = 4(N\lambda^2/2\pi)\,p_0\tan\frac{1}{2}\phi_2$	13.93(18)	14.12(25)	0.583(10)

[a]Small-angle prism has $\phi_1 = 31°56(2)'$ and large-angle prisms have $\phi_2 = 150°28(3)'$.

field gradient has been studied in an independent experiment[10] using the double-crystal spectrometer, with the results verifying the refractive index calculated from the interaction of the neutron magnetic dipole moment with the magnetic field. Refractive bending in the intense fields of the electromagnet was minimized in the present experiment by accurately centering the samples in the circular electromagnet gap. Since field refractive effects cancel for separations of the same spin state, correction was necessary for only one measurement and was found by measuring the angular shift of a polarized peak when the neutron spin was inverted by a radio-frequency coil in a Larmor precession field before passing through the magnetizing field in the empty gap of the electromagnet; it was less than 0.03 sec of arc.

The correction due to chemical impurities was simply calculated for the nuclear amplitude using known nuclear amplitudes. The correction to the magnetic amplitude was calculated assuming that Ni and Mn have magnetic moments of 0.6 and 3.0 μ_B, ferromagnetically aligned in the iron matrix and that the other impurities were nonmagnetic. The corrections were then

$$b(\mathrm{Fe}) = 1.0033b(\mathrm{meas}) - 0.0017\times10^{-12}\ \mathrm{cm/atom},$$

$$p_0(\mathrm{Fe}) = 1.0033p_0(\mathrm{meas}) - 0.0006\times10^{-12}\ \mathrm{cm/atom}.$$

IV. RESULTS

The results of the experimental determinations of the various refractive bending angles illustrated in Fig. 4 for the two experimental modes are summarized in Table I. From the various values of Δ, the values of the effective nuclear and forward magnetic scattering amplitudes for iron as used in the experiment can be obtained. These amplitudes were, from the small-angle prism data,

$$b(\mathrm{meas}) = 0.955(6)\times10^{-12}\ \mathrm{cm/atom},$$

$$p_0(\mathrm{meas}) = 0.590(6)\times10^{-12}\ \mathrm{cm/atom},$$

while those from the large-angle prism data were

$$b(\mathrm{meas}) = 0.952(10)\times10^{-12}\ \mathrm{cm/atom},$$

$$p_0(\mathrm{meas}) = 0.583(10)\times10^{-12}\ \mathrm{cm/atom}.$$

It is seen that these independent determinations agree comfortably within their standard errors. The resolution of the refracted peaks and the calibration of the goniometer were the major sources of uncertainty in the amplitude determination. The deviations from the ideal experiment were of comparable uncertainty, however, so that they too must be considered in any attempts to improve the precision beyond 1%. Combining the results of the two techniques and applying the composition correction, the amplitudes for pure iron are

$$b(\mathrm{Fe}) = 0.954(6)\times10^{-12}\ \mathrm{cm/atom},$$

$$p_0(\mathrm{Fe}) = 0.589(6)\times10^{-12}\ \mathrm{cm/atom}.$$

This value for the forward magnetic scattering amplitude agrees excellently with that calculated from the measured saturation magnetization. Using a very recent determination of the saturation magnetization at 28 °C, the temperature characteristic of the neutron experiment, by Crangle and Goodman[11] of 217.4 emu/g, one calculates 0.587×10^{-12} cm/atom for this scattering amplitude. It differs considerably from the value (0.645) which would be expected by extrapolation of the measured magnetic scattering amplitudes at Bragg reflections using theoretical wave functions for $3d$ electrons. This confirms the discrepancy previously noted and lends support to the existence of an anomalous magnetic form factor in iron in the small-angle region.

ACKNOWLEDGMENTS

We wish to thank Armand D'Addario for his skilled craftmanship in constructing the torsion goniometer and fabricating the prisms, Professor D. Shoemaker for the use of his optical goniometer, Professor A. Smakula for the use of his hydrostatic density measuring apparatus, Professor S. Moss for helpful discussions of lattice defects and annealing techniques, Art Gregor for his help in surface polishing and examination, and Don Guernsey for his chemical analyses of the samples.

---

*Research supported by the National Science Foundation, Washington, D. C.

†Present address: United States Naval Academy, Annapolis, Md. 21402.

[1]F. Bloch, Phys. Rev. 50, 259 (1936).

[2]C. G. Shull and Y. Yamada, J. Phys. Soc. Japan 17, 1 (1962).

[3]T. A. Kaplan, Phys. Rev. Letters 14, 499 (1965).

[4]R. E. Watson *et al.*, Phys. Rev. 139, A167 (1965).

[5]P. DeCicco and A. Kitz, MIT Solid State and Molecular Theory Group Quarterly Progress Report No. 63, 1967, p. 2 (unpublished).

[6]M. L. Goldberger and Frederick Seitz, Phys. Rev. 71, 294 (1947).

[7]O. Halpern, M. Hamermesh, and M. H. Johnson, Phys. Rev. 59, 981 (1941).

[8]The notation 2.393(3) used here gives the standard error with 68% probability in parentheses relative to the last significant figures.

[9]The first version of this instrument is described in C. G. Shull, K. W. Billman, and F. A. Wedgwood, Phys. Rev. 153, 1415 (1967).

[10]W. Just, C. S. Schneider, R. Ciszewski, and C. G. Shull (unpublished).

[11]J. Crangle and G. M. Goodman (unpublished).